Optics Communications 363 (2016) 37–41

Contents lists available at ScienceDirect

Optics Communications

journal homepage: www.elsevier.com/locate/optcom

Long-period grating assisted fractional differentiation of highly chirped light pulses

L. Poveda-Wong [a], A. Carrascosa [a], C. Cuadrado-Laborde [b,c,*], J.L. Cruz [a], A. Díez [a], M.V. Andrés [a]

[a] Departamento de Física Aplicada, ICMUV, Universidad de Valencia, Dr. Moliner 50, Burjassot E-46100, Spain
[b] Instituto de Física Rosario (CONICET-UNR), Blvr. 27 de Febrero 210bis, S2000EZP Rosario, Argentina
[c] Pontificia Universidad Católica Argentina, Facultad de Química e Ingeniería, Av. Pellegrini 3314, 2000 Rosario, Argentina

ARTICLE INFO

Article history:
Received 26 June 2015
Received in revised form
28 October 2015
Accepted 29 October 2015

Keywords:
Optical processing
All-optical devices
Pulse shaping

ABSTRACT

We experimentally demonstrate the possibility to perform a fractional differentiation of arbitrary order on a given light pulse by propagation through a single long-period grating. A simple analytical expression is obtained also, relating the fractional order of differentiation with the parameters of the long-period grating. A secant hyperbolic like pulse of 23 ps time width with a chirp parameter of −30 was successfully fractionally differentiated to the 0.5th order. The proposal was corroborated experimentally and numerically. The device may find applications in real time phase recovery.

1. Introduction

It is well-known that the inherent speed limitations of conventional electronics can be overcome by all-optical circuits, one of whose basic building blocks is a temporal differentiator. A photonic differentiator is a device that provides the time derivative of the complex envelope of an arbitrary input light pulse. The device may find interesting applications for optical pulse shaping, optical computing, information processing systems, and ultra-high-speed coding, among other uses. In the last few years different proposals were presented to perform photonic differentiation of integer order [1,2]. As far as we know, the first photonic fractional order differentiator was proposed in Ref. [3]. Since then, different solutions were found to perform photonic fractional differentiation by using asymmetrical π phase-shifted fiber Bragg grating [4], tilted fiber Bragg grating [5], silicon-on-isolator micro-ring resonators [6,7], and electrically tuned Mach–Zehnder interferometer [8]. Among them, the in-fiber solution offers some advantages, such as simplicity, low cost, low insertion loss, polarization independence, and inherent full compatibility with fiber optic systems. In Ref. [9] it was anticipated that a long-period grating (LPG) would provide the fractional order differentiation on an input light pulse propagating in the fundamental mode. However, nor an experimental analysis neither a theoretical expression relating the LPG characteristics with the fractional order of differentiation were provided.

In this work, we experimentally prove that a LPG can perform a 0.5th order fractional differentiation on an input light pulse. We also found a simple analytical expression relating the order of the fractional differentiation with the LPG characteristics. The effect of pre-chirping the input light pulse on the fractional differentiator output is also analyzed experimentally for the first time, as well as numerically. Very recently, it was shown that the signal's instantaneous frequency of an arbitrary light pulse can be obtained by simple dividing the temporal intensity profiles of the input and output of a spectrally shifted 0.5th order fractional differentiator [10]. Therefore, the 0.5th order fractional differentiator proposed here could found applications for simple real-time phase recovery purposes.

2. Theory

The Fourier transform $\Im$ of a signal $F(\omega)=\Im[f(t)]$ and its nth time derivative $F_n(\omega) = \Im[d^n f(t)/dt^n]$ are related by $F_n(\omega) = (j\omega)^n F(\omega)$, where $n \in R^+$, ω is the baseband angular frequency (i.e. $\omega=\omega_{opt}-\omega_0$, with ω_{opt} the optical angular frequency and ω_0 the carrier angular frequency), and $j=\sqrt{-1}$. Therefore we can consider the differentiation process as a filtering action performed by an ideal filter $H(\omega)$, with the transfer function:

$$H(\omega) = (j\omega)^n, \quad (1)$$

* Corresponding author at: Instituto de Física Rosario (CONICET-UNR), Blvr. 27 de Febrero 210bis, S2000EZP Rosario, Argentina.
E-mail address: Christian.Cuadrado@uv.es (C. Cuadrado-Laborde).

http://dx.doi.org/10.1016/j.optcom.2015.10.063
0030-4018/

on the input signal spectrum $F(\omega)$. It is worthwhile to mention that this necessarily implies a $n\times\pi$ phase discontinuity at ω_0, and a $|\omega|^n$ dependence for the amplitude, of the transfer function $H(\omega)$ [4].

An in-fiber LPG induces gradual coupling between the fundamental mode and co-propagating cladding modes as light propagates along the fiber length z. Unlike in FBGs, where there is a counter-propagating coupling between modes. The amplitude evolution of a pulse propagating in a LPG for both core and cladding modes can be described through the following matrix [11]:

$$\begin{bmatrix} A_1(z,\omega) \\ A_2(z,\omega) \end{bmatrix} = \begin{bmatrix} F_{11}(z,\omega) & F_{12}(z,\omega) \\ F_{21}(z,\omega) & F_{22}(z,\omega) \end{bmatrix} \begin{bmatrix} A_1(0,\omega) \\ A_2(0,\omega) \end{bmatrix}, \tag{2}$$

where $A_i(0,\omega)=\mathfrak{I}[a_i(0,t)]$, and $a_i(0,t)$ is the temporal amplitude of the pulse at the beginning of the LPG ($z=0$) and the sub-index $i=1$, 2 denotes the core and cladding modes, respectively. If the index modulation depth and the periodicity are constants over the whole grating, each matrix element in Eq. (2) has the following expressions:

$$\begin{aligned} F_{11}(z,\omega) &= \left[\cos(\gamma z) + j\sigma\gamma^{-1}\sin(\gamma z)\right]\exp\left[j(\beta_1-\sigma)z\right], \\ F_{12}(z,\omega) &= j\kappa\gamma^{-1}\sin(\gamma z)\exp\left[j(\beta_1-\sigma)z\right], \\ F_{21}(z,\omega) &= j\kappa\gamma^{-1}\sin(\gamma z)\exp\left[j(\beta_2+\sigma)z\right], \\ F_{22}(z,\omega) &= \left[\cos(\gamma z) - j\sigma\gamma^{-1}\sin(\gamma z)\right]\exp\left[j(\beta_2+\sigma)z\right], \end{aligned} \tag{3}$$

where κ is the coupling coefficient, $2\sigma(\omega)=\beta_1(\omega)-\beta_2(\omega)-2\pi/\Lambda$, $\beta_1(\omega)$ and $\beta_2(\omega)$ are the propagation constants for the core and the cladding modes, respectively; Λ is the grating period, and $\gamma^2=\kappa^2+\sigma^2$ [11]. In the following, we will find an analytical expression relating the fractional order of differentiation n with the LPG parameters.

If only the fundamental mode is initially excited by the pulse launched at the input of the LPG, i.e. $A_2(0,\omega)=0$, see Eq. (2). Then the temporal pulse envelope propagating through the core at a distance z along the LPG can be obtained by $a_1(z,t)=\mathfrak{I}^{-1}[A_1(z,\omega)]=\mathfrak{I}^{-1}[F_{11}(z,\omega)\,A_1(0,\omega)]$, see Eq. (2), where $\mathfrak{I}^{-1}$ stands for the inverse Fourier transform. In this sense, $F_{11}(z,\omega)$ can be considered the transfer function $H(\omega)$ of our device; whose phase will be given by:

$$\theta(\gamma) = \frac{\pi}{2}\,\mathrm{sgn}\left[\frac{\sigma}{\gamma}\sin(\gamma z)\right] - \arctan\left(\frac{\gamma}{\sigma}\cot(\gamma z)\right) + (\beta_1-\sigma)z, \tag{4}$$

where sgn[.] is the signum function. In the following, and only for simplicity, the term $\beta_1 z$ will be omitted in Eq. (4), since it is only responsible of a time delay in the output signal. The maximum phase change $\Delta\theta$, can be obtained by finding the roots of the first derivative of Eq. (4), which are given by $\gamma z=\pi/2$. By replacing this value in Eq. (4) and taking into account that $\Delta\theta=n\times\pi$, we arrive to an analytical expression for n as a function of the LPG parameters:

$$n = 1 - \sqrt{1-(z/L)^2}, \tag{5}$$

where L is the LPG length providing full-energy coupling into the cladding mode, i.e. $\kappa L=\pi/2$. The simplicity of this expression is remarkable, especially when taking into account that no approximation was used. It is worth to mention also, the generality of expression given by Eq. (5), i.e., every LPG designed to perform a full-energy coupling into the cladding mode, behaves as a fractional order differentiator at fractions of its characteristic grating length L. Being the fractional order n only related with this fraction of the grating length. When $z=L$, $n=1$, see Eq. (5); and in this situation the phase shift $\Delta\theta=\pi$, and the transmission varies linearly with the baseband frequency around $\omega=0$, as it is required for a first order differentiator [2]. On the other hand, at fractions of L, the spectral behavior approaches that of a fractional order differentiator; i.e., with a maximum phase change within a narrow spectral bandwidth and a transmission dip at $\omega=0$. In this way, an optical pulse propagating in the core mode of a LPG designed for full-energy coupling ($\kappa L=\pi/2$) experiences all the fractional derivatives between $n=0$ (for $z=0$) and $n=1$ (for $z=L$) while propagates through the LPG. Finally, the maximum operative optical bandwidth of the LPG working as a fractional order differentiator is determined by the first transmission maxima at both sides of the resonance dip. The solution can be found by solving $|F_{11}(z,\omega)|=1$, see Eq. (3), which is given by $\gamma z=\pi$.

3. Results

Fig. 1(a) shows graphically the relationship given by Eq. (5). The amplitude and phase responses of the LPG are shown in Fig. 1 (b) and (c), at different fractions of the LPG length given by $z/L=1$, 0.954, and 0.866. By using Eq. (5), these fraction lengths corresponds to the following fractional differentiator orders $n=1$, 0.7, and 0.5, respectively. This simulation of the LPG was performed by using the same parameters described in Ref. [9]. For example, when $z/L=0.866$ ($n=0.5$), the maximum phase change is $\Delta\theta=1.57$ rad, see the dotted lines in Fig. 1(c), which match exactly with the expected phase change of a 0.5th order fractional differentiator $\Delta\theta=0.5\times\pi=1.57$ rad.

The experimental setup is shown in Fig. 2. Since we test chirped light pulses, we found essential to monitor its instantaneous angular frequency profile before and after the fractional order differentiation. To this end, we will use the phase recovery technique presented in Ref. [12] for this specific task. The original signal $f(t)$, as well as the fractionally differentiated signal $d^n f(t)/dt^n$, are split by an optical fiber coupler, and further propagated along a fiber spool. Then, the intensity profiles of both the un-propagated and propagated signals are registered by $a>63$ GHz sampling oscilloscope provided with a fast built-in photodetector (53 GHz), in both cases. The propagation was performed in a low numerical aperture optical fiber (SM980 by Fibercore), whose length was of 44 m in both cases. The measured first-order dispersion of this optical fiber is -44 ps/nm × km, at the emission wavelength of the laser that we used in our experiments. The LPG was inscribed in a boron doped photosensitive fiber (PS980 by Fibercore, numerical aperture of 0.13 and a cut-off wavelength of 980 nm) by using the point-by-point technique. The selected periodicity was of 187.6 μm, with a final LPG length of 146.5 mm. The transmission response of the LPG was followed during the fabrication process by recording the transmitted light provided by a led source in an optical spectrum analyzer. We interrupted the LPG fabrication when the transmission reached a resonance depth of 14 dB at 1042.549 nm with a 3 dB bandwidth of 1.14 nm. This resonance depth is below the full coupling condition, being equivalent to a working condition of $z/L\cong0.86$, which in turn corresponds to a 0.5th order fractional differentiator, see Fig. 1(a). The light pulses to be optically differentiated were provided by a passively mode-locked ytterbium fiber laser, emitting at a fixed wavelength $\lambda_0=1038.5$ nm. The LPG was carefully tuned to the central wavelength of the laser through a micrometric translational stage. The spectrum of the LPG, after the wavelength tuning, can be observed in Fig. 3(a). In the same figure, the theoretical intensity response of an ideal 0.5th order fractional differentiator was superimposed. The degree of similarity between both is reasonably good within the whole operative optical bandwidth, except at the resonance frequency, where the theoretical transmission decay to $-\infty$ (as opposed to our LPG which decays to -14 dB). However, as it has been discussed before [13], a slight

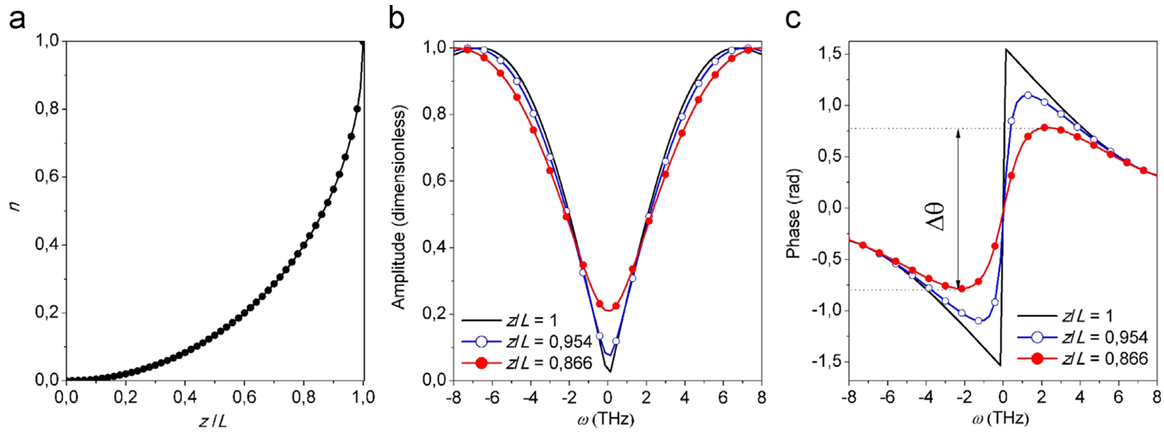

Fig. 1. (a) Fractional order of differentiation n as a function of the grating length z/L. (b) Amplitude and (c) phase response of the LPG at different fractions of the grating length.

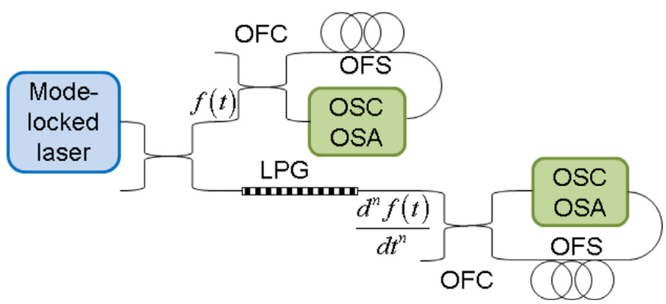

Fig. 2. Experimental setup for fractional order differentiation with a LPG, where OFS, OFC, OSC, and OSA stands for optical fiber spool, optical fiber coupler, oscilloscope, and optical spectrum analyzer, respectively.

deviation in the magnitude response of the proposed filter to perform the fractional differentiation (as compared with the ideal filter) has lower consequences that the same deviation in the phase response. This difference between the ideal fractional order differentiation and the (approximate) fractional order differentiation performed by a LPG is finally a function of the input bandwidth. However, the deviation between both can be minimal, when the input bandwidth is adequately selected [9]. The repetition rate of the mode-locked laser was of 23.15 MHz, and the output light pulses can be approximately fitted with an hyperbolic secant profile $f(t)=\text{sech}(t/T_0)$, with $T_0=13$ ps, i.e., a FWHM of 23 ps, see Fig. 3(b). Fig. 3(c) shows the spectra of the signals at the input and output of the LPG. One can see that the input signal

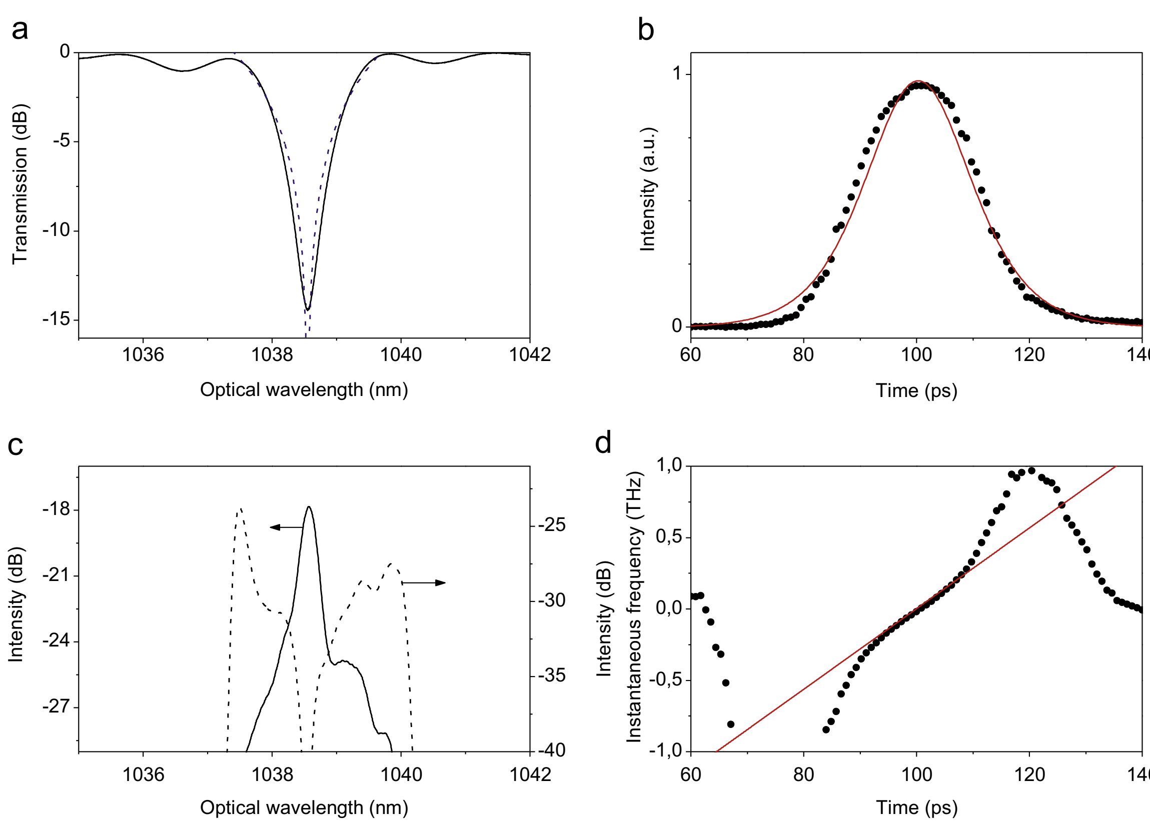

Fig. 3. (a) Measured optical spectrum of the LPG and theoretical intensity response of a 0.5th order fractional differentiator, solid and dashed lines, respectively. (b) Measured output light pulse of the mode-locked laser with its corresponding fitting, scatter points and solid curve respectively. (c) Measured spectra of the light pulses at the input and output of the LPG, solid and dotted lines, respectively. (d) Measured instantaneous frequency of the output light pulse of the mode-locked laser, with its corresponding linear fitting with $C=-30$, scatter points and solid curve, respectively.

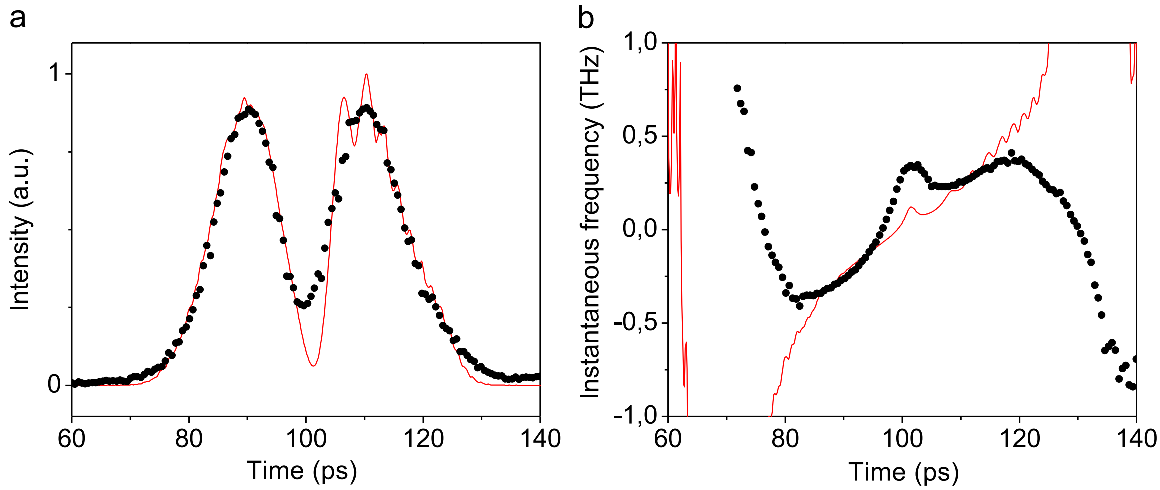

Fig. 4. (a) Measured temporal intensity profile of the light pulse at the output of the LPG and simulated response of an ideal 0.5th order fractional differentiator, scatter points and solid curve, respectively. (b) Measured instantaneous frequency of the light pulse at the output of the LPG and calculated instantaneous frequency for the simulated response of an ideal 0.5th order fractional differentiator, scatter points and solid curve, respectively.

carrier is well aligned with the resonance optical wavelength of the LPG – compare with the resonance dip shown in Fig. 3(a) – as a result, the optical carrier is deeply suppressed at the output spectrum, as expected for a photonic differentiator, regardless being fractional or not. The instantaneous frequency of $f(t)$ was measured by using the temporal intensity profiles of both the original and propagated pulses registered by the oscilloscope, see Fig. 3(d) – the details of this technique can be followed in Ref. [12]. The measured instantaneous frequency increases monotonously from the leading to the trailing edge of the pulse; which is currently known as an up-chirp. We emphasize that we should focus our attention to the region where the pulse energy is localized, see Fig. 3(b). Therefore, the measured instantaneous frequency profile of the input pulse $f(t)$ can be fitted linearly, see Fig. 3(d). This implies a parabolic phase profile for the output pulse of the mode-locked laser $f(t)$, which can be approximately described by $\exp(-jCt^2/2T_0^2)$, where C is the chirp parameter, being $C=-30$ according to our fitting.

Fig. 4(a) shows the measured temporal intensity profiles of the light pulse at the output of the LPG. In the same figure, it is also shown the simulated response of an ideal 0.5th order fractional differentiator; by composing an input pulse with the square root of the measured temporal intensity profile as the modulus, and the reconstructed phase obtained above for $f(t)$. The sinusoidal ripple superimposed in the simulated pulse – much more evident in the right peak; is a consequence of a constructive interference because of the spectrum splitting after the optical differentiation. This is exclusive of highly chirped pulse differentiation, and it was not detected in the measured pulse because of insufficient bandwidth in our available detectors. The instantaneous frequency of the light pulses at the output of the LPG, i.e., $d^n f(t)/dt^n|_{n=0.5}$, was measured by using the temporal intensity profiles of both, the originally fractional differentiated and further propagated pulses registered by the oscilloscope, see Fig. 4(b). In the same figure, we also have shown a calculated instantaneous frequency for the simulated response and propagation of the ideal 0.5th order fractional differentiator, shown in Fig. 4(a). The peak in the instantaneous frequency profile corresponding to the intensity minima between the peaks of intensity maxima (localized at ~100 ps), is a consequence of the phase difference $\Delta\theta=0.5\times\pi$ between the right and left peaks of the differentiated pulses, which in turn is a consequence of the fractional differentiation, see Fig. 4(b). It is interesting to point out that if the LPG would have a frequency response of the type $H(\omega)=|(j\omega)^n|$ – i.e., similar only in intensity to a fractional order differentiator filter response, but without a phase discontinuity at the resonance frequency; the measured instantaneous frequency profile would be linear, i.e., without an instantaneous frequency peak in the intensity minima between the peaks of intensity maxima.

Next, we further corroborate the order of the experimental fractional differentiation performed ($n=0.5$), by comparing with the simulated response of two different ideal fractional order differentiators with orders $n=0.2$ and $n=\mathbf{0.8}$, see Fig. 5(a). In these simulations we composed an input pulse with the square root of the measured temporal intensity profile as the modulus, and the measured phase obtained for $f(t)$, as we did for the results shown in Fig. 4. Two main features can be distinguished, first the temporal separation between intensity peaks increases directly with the fractional order, from 13 ps ($n=0.2$), to 24 ps ($n=1$); as compared with the measured temporal separation of 19 ps ($n=0.5$). Second the intensity minima, which is located between intensity maxima, decreases as the fractional order increases, eventually reaching zero when $n=1$. On the contrary, the waveform of the fractionally differentiated pulse remains practically unchanged.

We conclude by showing the effect of chirp on the fractionally differentiated signal. In Fig. 5(b) we show the simulated response of an ideal 0.5th order fractional differentiator when the simulated signal is chirp free, and twice chirped, i.e. $C=0$ and $C=-60$, as compared with the measured temporal intensity profiles of the light pulse at the output of the LPG (where the measured chirp $C=-30$). Not only the waveform of the composed twin pulse, but its temporal width changes, decreasing inversely with the degree of chirp, from 46 ps ($C=0$), to 25 ps ($C=-60$); as compared with the measured temporal separation of 35 ps ($C=-30$). Thus, this parameter could be used as a simple technique to rapidly estimate the degree of chirp (especially for single-shot non-repetitive signals); being minimum the chirp when the temporal width of the differentiated pulse is maxima.

4. Conclusions

In this work we experimentally prove that a LPG can perform a fractional order differentiation on an input light pulse propagating by the fundamental mode. A simple analytical expression was found relating the order of the fractional differentiation with the characteristics of the LPG. A LPG provides the simplest technique to perform a photonic fractional differentiation. Further work is in

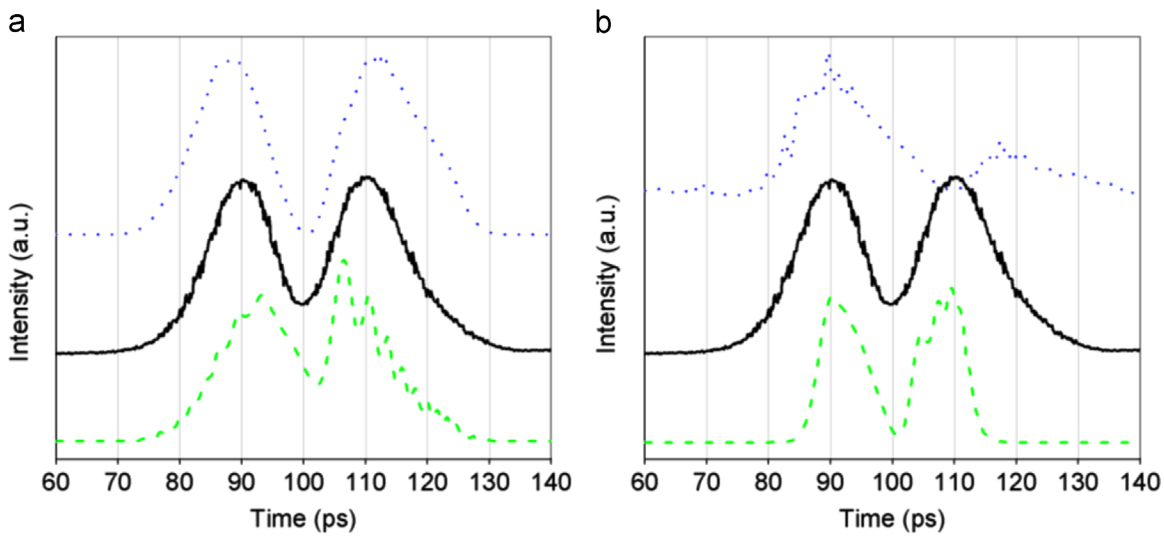

Fig. 5. (a) Measured temporal intensity profile of the light pulse at the output of the LPG (solid curve), and simulated responses of an ideal 0.2th and 0.8th order fractional differentiator, dashed and dotted curves, respectively. (b) Measured temporal intensity profile of the light pulse at the output of the LPG (solid curve) and simulated responses of an ideal 0.5th order fractional differentiator when the input pulse is chirp free and twice chirped as considered in the example shown in Fig. 4(a), dotted and dashed curves, respectively.

progress to use this device for phase recovery purposes.

Acknowledgments

The authors acknowledge financial support from the Ministerio de Economía y Competitividad of Spain and the Fondo Europeo de Desarrollo Regional (FEDER) – Project TEC2013-46643-C2-1-R – and the Generalitat Valenciana – Project PROMETEOII/2014/072. L. Poveda-Wong acknowledges financial support from the Generalitat Valenciana (Ref.: GRISOLIA/2013/001).

References

[1] N. Berger, B. Levit, B. Fischer, M. Kulishov, D. Plant, J. Azaña, Temporal differentiation of optical signals using a phase-shifted fiber Bragg grating, Opt. Express 15 (2007) 371–381.
[2] R. Slavík, Y. Park, M. Kulishov, R. Morandotti, J. Azaña, Ultrafast all-optical differentiators, Opt. Express 14 (2006) 10699–10707.
[3] C. Cuadrado-Laborde, All-optical ultrafast fractional differentiator, Opt. Quantum Electron 40 (2008) 983–990.
[4] C. Cuadrado-Laborde, M.V. Andrés, In-fiber all-optical fractional differentiator, Opt. Lett. 34 (2009) 833–835.
[5] M. Li, L.-Y. Shao, J. Albert, J. Yao, Continuously tunable photonic fractional temporal differentiator based on a tilted fiber Bragg grating, IEEE Photon. Technol. Lett. 23 (2011) 251–253.
[6] H. Shahoei, D.-X. Xu, J.H. Schmid, J. Yao, Photonic fractional-order differentiator using an SOI microring resonator with an MMI coupler, IEEE Photon. Technol. Lett. 25 (2013) 1408–1411.
[7] A. Zheng, J. Dong, L. Zhou, X. Xiao, Q. Yang, X. Zhang, J. Chen, Fractional-order photonic differentiator using an on-chip microring resonator, Opt. Lett. 39 (2014) 6355–6358.
[8] A. Zheng, T. Yang, X. Xiao, Q. Yang, X. Zhang, J. Dong, Tunable fractional-order differentiator using an electrically tuned silicon-on-isolator Mach–Zehnder interferometer, Opt. Express 22 (2014) 18232–18237.
[9] C. Cuadrado-Laborde, M.V. Andrés, Design of an ultra-broadband all-optical fractional differentiator with a long-period fiber grating, Opt. Quantum Electron 42 (2011) 571–576.
[10] C. Cuadrado-Laborde, M.V. Andrés, J. Lancis, Self-referenced phase reconstruction proposal of GHz bandwidth non-periodical optical pulses by in-fiber semi-differintegration, Opt. Commun. 284 (2011) 5636–5640.
[11] T. Erdogan, Fiber grating spectra, J. Lightwave Technol. 15 (1997) 1277–1294.
[12] C. Cuadrado-Laborde, A. Carrascosa, P. Pérez-Millán, A. Díez, J. Cruz, M. Andres, Phase recovery by using optical fiber dispersion, Opt. Lett. 39 (2014) 598–601.
[13] A.V. Oppenheim, J.S. Lim, The importance of phase in signals, Proc. IEEE 69 (1981) 529–541.